

Paper No.2

ADVANCED TECHNOLOGY APPLIED TO THE
UH-60A AND S-76 HELICOPTERS

WILLIAM F. PAUL, DIVISION VICE-PRESIDENT, ENGINEERING

AND

ROBERT ZINCONE, CHIEF ENGINEER

SIKORSKY AIRCRAFT
DIVISION OF UNITED TECHNOLOGIES CORPORATION
STRATFORD, CONNECTICUT

JULY 1977

PREPARED FOR PRESENTATION AT THE
"THIRD EUROPEAN ROTORCRAFT AND POWERED
LIFT AIRCRAFT SYMPOSIUM"
SEPTEMBER 7 -9, 1977, AIX-EN-PROVENCE, FRANCE

The U.S. Government does not attest to the accuracy of this information or the corporate views expressed therein. Approval to present this paper was based on this condition. (Export license No. 042293)

ADVANCED TECHNOLOGY APPLIED TO THE
UH-60A AND S-76 HELICOPTERS

Introduction

We are at the threshold of a new era in the production of helicopters which were spawned by the advanced technology developed during the past decade. This technology was acquired in response to a need to bring the helicopter to the maturity desired for so long by the operators — both military and commercial. Looking back briefly over the history of development we can observe the decade of the 1940's as a period in which basic concepts were explored as exemplified by the Sikorsky VS-300, Figure 1, and in which various ideas for control were evaluated using ground test vehicles such as the simulator used by Mr. Sikorsky, Figure 2. The decade of the 1950's saw large production and expanded application of helicopters in military and commercial roles, Figure 3. This broadened use exposed many problems resulting from the various operational environments encountered such as blade erosion and corrosion of components and demonstrated the need to reduce component fatigue due to vibratory loadings. Many of these problems were solved in the decade of the 1960's and the helicopter established itself as a viable product. Decisions were made during this period on such questions as in which direction to rotate the tail rotor, whether to use grease or oil lubrication, whether to use fixed or free turbines, how much authority to build into the stability augmentation system, how to reduce vibration levels, and many more. This decade saw the S-61, S-64 and S-65 turbine helicopters in production, Figure 4. The promise of the 1960's gave rise to accelerated research and development beginning about 1965 and extending for approximately a decade in which dramatic breakthroughs in analysis and materials applications and in aerodynamics and dynamics technology were achieved. This research and development established the technology base for meeting the challenge of the 1970's and 1980's.

This paper is directed towards the specific technology developed and implemented on the UH-60A and S-76 helicopters.

UH-60A and S-76 Advanced Technology

The advanced technology applied to the UH-60A is illustrated in Figure 5 and includes a composite titanium spar highly twisted rotor blade with advanced airfoils and swept tip, a forged titanium hub elastomeric main rotor, a canted, bearingless graphite tail rotor, self-tuned bifilar vibration absorber, modularized transmission system, digital electronic automatic flight control system, an automatically programmed stabilator and broad use of organic materials in the airframe. In addition to these features the UH-60A was designed to provide crashworthiness and ballistic survivability.

The major advanced technology features of the S-76 helicopter are shown in Figure 6, most of which are common to the UH-60A.

Before proceeding with the technology discussion we will review briefly the design requirements of these helicopters.

UTTAS Design Requirements

The reader is referred to a paper presented by Gormont and Wolfe at the AGARD Rotorcraft Symposium, Reference (a) which presents a detailed discussion of the Army requirements for the Utility Tactical Transport Aircraft System. The critical requirements include vertical climb of 450 fpm at 4000 ft., 95°F temperature with full load and at 95% rated power, maximum cruise speed of 145-175 knots, crashworthiness in a 42 ft/sec vertical landing impact, zero vulnerable area to 7.62 mm projectiles, system mean time between failure of 4.5 hours, 0.8 maintenance man-hours per flight hour in the field, air transportability in the C-130 and design to specified cost.

S-76 Design Requirement

The basic requirement for the S-76 is to carry 12 passengers and a crew of two on a 400 n. m. mission at a gross weight under 10,000 lbs. and at 3000 ft. ISA. The aircraft must operate IFR Category A, with a cruise speed of 145 knots, SL STD and be equipped with flotation gear. Cost targets were established to provide a 2/3 reduction of acquisition cost relative to the S-61 and 30% lower direct operating cost.

These requirements made it clear that our task at Sikorsky was to achieve a major improvement in figure-of-merit and to achieve forward flight speed requirements with no structural limits. Also to make major improvements in structural efficiency to meet weight targets and to achieve the cost, R&M and survivability requirements.

Rotor Technology

The achievement of better hover capability is still "the name of the game". We found that we would need 18° of blade twist with thinner, cambered airfoils to obtain a sufficient increase in hover efficiency to offset approximately 1000 lbs. of weight increases that were expected to meet the crashworthiness, survivability and de-icing requirements of the UH-60A. Figure 7 shows how the increased hover efficiency was used to offset these weight increments. How was this achieved?

Over the past decade the hover performance of helicopters has been progressively improved, largely through a better understanding of the role that the vortex wake shed by the blades plays in shaping the inflow velocity distribution. Flow visualization pictures taken using Schlieren optical techniques or smoke, Figure 8, showed that the tip vortex was not, as had been previously believed, swept away from the plane of the blades but was held up, passing very close under the following blade. This close passage, and the resulting high angles of attack induced over those portions of the blade outboard of the vortex, led to blade stall

and high power consumption on the low twist blades in common use at the time. The use of higher twist, especially in the tip region, reduces the extent of the stall induced by the interfering vortex while at the same time providing a distribution of blade loading that is closer to optimum, both resulting in lower power required. This is reflected in the trend of improving figure-of-merit (hover efficiency) with increased twist shown in Figure 9. With the choice of high twist for the UH-60A it now became necessary to develop the technology to make a high twist rotor work in all flight regimes. This will be discussed later.

One of the most important refinements added to the analysis used to calculate rotor performance in forward flight has been the ability to model inflow velocity distributions more representative of the real world flow field than the constant induced velocity (inflow) assumed in earlier analyses. In the 1960's we discussed this at many symposia but in the UH-60A and S-76 this was applied in design and had a profound effect on the rotor geometry and particularly the airfoil selection. This is important since with a realistic indication of the inflow velocity the true aerodynamic angle of attack of the blade sections can be calculated. Not only was the analysis developed but the effects were proven in numerous tests. An example of how important this is is shown in Figure 10, where angle of attack contours for the same rotor calculated using the two inflow assumptions are compared. It can be seen that the constant inflow rotor has undesirable negative angles of attack at the tip of the advancing blade and a comparatively benign retreating blade environment. This contrasts with the variable inflow calculation which has a well behaved advancing blade and large pockets of stall in the third and fourth quadrants. Airfoil selection based on the constant inflow picture would result in a choice quite different from that required to provide good performance in the variable inflow "real" world.

As a result of being able to define the rotor blade operating environment more precisely it was possible to tailor the airfoil to the flow conditions at a particular spanwise location. For rotors such as those of the UH-60A and the S-76, efficient operation demands a tip section with good high speed characteristics, for low drag at low lifts on the advancing blade, combined with effective performance at the intermediate lifts and Mach numbers typical of the outer blade sections on the hovering rotor. Sections inboard, which approach stall on the retreating blade, must have good maximum lift capability. To achieve these goals the advanced Sikorsky rotors use combinations of two airfoils, the SC-1095 with good mid and high Mach number performance, and the SC-1095 R8, specially designed to provide high maximum lift without paying a penalty in increased drag or pitching moment. These airfoil profiles were designed after thorough studies showed that existing conventional and laminar flow airfoils would not provide the required aerodynamic characteristics. Patents were obtained for these profiles. Figure 11, comparing the variation of CL_{MAX} with Mach Number, shows how the performance of the two sections are tailored for the speed range of interest.

The combination of airfoils specially chosen to match their environment with optimum performance push the operating envelope of the Sikorsky advanced titanium technology rotors, as represented by the UH-60A, well beyond that of the aluminum technology rotor aircraft it replaces in the Army inventory. Figure 12 highlights this where the gross weight, speed envelope of the titanium technology rotor is compared with that of today's aluminum rotor system.

Another benefit of the improved understanding of the rotor flow environment and the advanced analytic tools available to the designer is a new flexibility in tip design options. Apart from the dynamic benefits of tip sweep noted above, tip sweep provides Mach Number relief to the advancing blade tip at high cruise speeds. This has performance and reduced drag benefits and, because shock strengths are reduced, pronounced acoustic benefits. Being able to dissect performance in detail in the design stages allows trades to be made between advancing blade and retreating blade drag and for certain applications where high retreating blade tip loads are not carried, for instance in civil aircraft with low maneuver requirement, taper can have a beneficial effect.

Numerous flight experiments of twisted blades were performed to search for means to extend the speed limitations encountered in forward flight. These limitations included the high build-up of blade stresses and control system vibratory loadings and the presence of subharmonic blade flapping caused by coupling of blade flapwise bending and torsion and also evidence of stall flutter. These conditions were aggravated in forward flight by use of high twist. The high twist of the blade causes the advancing blade tip to bend downward. As a result the drag force at the tip creates a nose down pitching moment which causes negative twisting and further downward bending. This effect is illustrated in Figure 13. This led to the development of the swept tip on the Sikorsky S-67 BLACKHAWK which met with immediate success. The reduction in torsional response of the swept tip blades improves blade tracking at high speed flight. This effect is shown in Figure 14 which shows the reduction in the difference in pitch angles of the blades at an advance ratio of 0.35 as a function of blade torsional stiffness. The swept tip also reduces vibratory controls loads. The benefits measured in flight tests of the CH-54B helicopter are illustrated in Figure 15.

The tip configurations have been improved since the early demonstrations. The UH-60A blade planform is shown in Figure 16. The outer 7 percent of the blade is swept back 20 degrees and the total twist is 18 degrees. The S-76 blade, shown in Figure 17, uses 10 degrees of twist and has a swept tapered tip over the outer 9.5 percent of the blade. Tests of a series of tips in the NASA-Ames 40 x 80-foot tunnel showed that a tip with combined taper and sweep reduced the power required at cruise speeds below that of constant chord swept tips and even more so for unswept tapered and constant chord tips. The differences in power required are shown in Figure 18.

Blade Structural Design

Given the geometry required to meet performance specifications the task now becomes the design of a structure which will provide no restrictions of any kind throughout the helicopter flight envelope and that would meet Sikorsky design criteria for reliable mass produced blades. The key to success was to make the right choice of materials for the right application. The result was a blade structure which is truly a composite of materials: Kevlar[®] tip, fiberglass skin, Nomex[®] honeycomb trailing structure, graphite trailing edge, fiberglass leading edge counterweight, titanium spar and abrasion strip and a redundant graphite root end. The blade structure is shown in Figure 19. Why was titanium selected for the primary structure of the blade as opposed to fiberglass or graphite? Titanium was the only material that provides all of the following:

- a) the high bending fatigue strength to allow use of high twist blades;
- b) the high torsional stiffness-to-weight ratio that allowed a weight-efficient, stable design;
- c) the degree of technology readiness required for commitment of major resources to a new production main rotor blade design;
- d) competitive costs.

Graphite composites were eliminated on the basis of item (c) and (d) while fiberglass was eliminated on the basis of item (b) as discussed below.

Figure 20 shows that high twist blades require a high strength material if forward flight performance is not to be compromised. Titanium, fiberglass and graphite all offer significant advantages over aluminum in this respect and all can meet the bending strength requirement. Torsional stiffness requirements, therefore, became the determining factor. Cambered, high-twist blades generate greater aerodynamic twisting moments in forward flight, Figure 21. Unless stringent torsional stiffness design criteria are imposed, advancing blade instability problems can result. Track and balance can also be compromised to the point where undesired vibration exists and blade interchangeability is lost. Figure 22 shows the growth in elastic twist with speed for blades of comparable weight but made of different candidate materials. The reason for choosing titanium for the high twist cambered blade is apparent.

Rotor blade reliability is an equally important design issue. The safety or reliability of a rotor blade, as with any other structural component, is directly a function of the stress derating used. This is as true for composite structures as it is for metal structures; they all are susceptible to manufacturing, material and service-induced flaws that will degrade their basic strength. Many of the metal spar rotor blades in existence today were not adequately derated resulting in service problems because of the low tolerance of the blades

to flaws such as those due to corrosion. Sikorsky's titanium rotor blades have been derated by a factor twice as large as our previous, very successful aluminum blades, Figure 23, to a level that has been demonstrated to be adequate by service testing (for tens of millions of hours) of rotor components and other non-redundant metal components such as main rotor shafts. Figure 24 shows the perfect record achieved on aluminum blades in areas where stress levels meet this derating criteria. On the S-76, our titanium spar operates at less than 1/3 of its mean strength — well below the requirements, Figure 25. To further justify this position hundreds of titanium specimens with severe artificially induced defects have been fatigue tested. None of these defects would reduce the spar strength below its operative stresses. In addition to the basic reliability provided by the stress derating possible with titanium, materials in our titanium and fiberglass blade will not corrode. Finally, the titanium spar is encased in the fiberglass skin to protect it from foreign object damage.

Sikorsky's decision to use the titanium/composite main rotor blade reflects a careful consideration of all these factors. The titanium spar is used because it provides the stiffness, strength and proven source reliability that no other material can provide now or in the near future. The thin composite skins and graphite trailing edge spline are secondary structures and are readily inspectable due to their thinness and provide a significant decrease in weight and increase in blade reliability when compared with the thin metal skins used on earlier rotor blades.

Remaining critical issues addressed in the selection of our design approach are those of survivability and of cost. Ballistic tests have demonstrated that the titanium spar can meet the Army UTTAS 7.62 requirement. Further, the spar is tolerant to many types of 23 mm strikes — particularly the highly probable strike from the leading edge or trailing edge direction, Figure 26.

Elastomeric Rotor — The main rotor achieves its high reliability and low maintenance through the use of elastomeric bearings in a unique Sikorsky patent configuration. These elastomeric bearings support the full centrifugal load generated by each rotor blade, and provide universal freedom for the blade pitch, flap, and lead/lag motions which occur once per revolution in a fully articulated rotor. Since these bearings accommodate motion by simple flexing of their elastomer laminates, there are no rolling or sliding elements as in more conventional bearings. No lubrication or servicing of any kind is required. Seals, boots, or dust covers are not needed and there is no friction or wear. The result is a bearing system which provides extremely long life, and which requires no maintenance of any kind. In addition, a simple visual inspection of the bearing's surface at periodic intervals is sufficient to determine the bearing's condition. This feature of elastomeric bearings provides the basis for the "on condition" replacement philosophy applied to the UTTAS main rotor. There is no scheduled overhaul interval. These bearings are simply replaced as required throughout the life of the helicopter. The unique UH-60A rotor is designed to permit easy replacement of these bearings in the field without removal of the rotor or disassembly of any major components.

A thrust bearing, constructed of essentially flat laminates, cooperates with the spherical bearing at each blade root, Figure 27. These two bearings combine to react all blade loads and motions. The spherical elastomeric bearing is primarily designed to accommodate all the blade flap and lag motions, while the elastomeric thrust bearing is designed to accommodate most of the imposed blade pitch motion. Both bearings react full blade centrifugal force, but they share blade pitch motion in a ratio inversely proportional to their respective stiffnesses, acting as two torsional springs in series. This sharing results in a spherical bearing of minimum diameter, which is a major design consideration in obtaining the smallest possible hub enclosure to contain the elastomeric bearing. The resultant UTTAS rotor system design, is lighter in weight, lower in cost, and has greater reliability than conventional articulated rotor systems. The compactness of the UH-60A design is evident in Figure 28.

The elastomeric bearing manufacturers, Lord Kinematics and C/R Industries have contributed greatly to the successful development of Sikorsky's elastomeric rotor. They have developed materials and processes which provide higher and more uniform material strain allowables, higher bond strengths, greater resistance to temperature extremes, and better endurance under many hostile environments. Bearing designs have been produced which incorporate such features as graduated metal shim spacing and a regulated elastomer modulus distribution, in order to equalize bearing strain distributions. To optimize such bearing designs, and to analyze the more complex laminated structures, computerized finite element analytical programs were developed with which the hydrostatic pressure in the elastomer laminates under load can be computed. The distribution of this pressure across each laminate and the variation in this distribution as the load is moved can be determined. The elastomer bulge and shear strains due to elastomer pressure and metal shim stresses due to shim bending as the elastomer pressure fluctuates can be calculated. The steady and vibratory stresses and strains are used in determining the projected bearing performance when compared to known material allowables.

The UTTAS elastomeric bearings are designed to have a 2000 hour B₁₀ life. This level of reliability far exceeds that attainable with conventional lubricated or non-lubricated rotor bearing systems. These elastomeric bearings have undergone extensive testing to verify that they surpass their design life requirements.

An important element in the development of the elastomeric rotor was the design of a suitable elastomeric bearing test and qualification facility. The test apparatus shown in Figure 29 was designed for fatigue testing the bearing under the full spectrum of flight loads and deflections. This permitted a reliable qualification of the bearings.

Damper Design — The damper proved very effective in handling the onset of harmonics at high speeds caused by engine drive system coupling which were related to flap-lag and collective modes (2 Hz, 2-1/2 P, etc.). The classical role of the lag damper in an articulated rotor design is to provide sufficient damping to preclude ground resonance. In this respect the damper has served its purpose in the advanced technology UH-60A and S-76 designs. With the continuing improvement in engine responsiveness, system transient response and rotor droop characteristics, through engine and fuel control design, a second vital role has emerged for the lag damper. The damper must also provide sufficient damping to achieve adequate coupled rotor/drive system torsional mode stability. The engine and fuel control are purposely designed so that they are very responsive and thus add energy to the system at the rotor/drive system torsional mode frequency. As illustrated in Figure 30, the excellent torsional stability of the UH-60A and S-76 systems is a direct result of the damping provided by the blade lag dampers.

The Canted Bearingless Tail Rotor

The tail rotor system is a simple bearingless/hingeless design using composite blades and titanium hub plates to reduce the number of parts required to one third those of a conventional rotor, Figure 31. A graphite spar that is continuous from one blade through the center hub to the opposite blade, is used to provide both pitch and flap motion without hinges and bearings. The unique properties of graphite composite allow a low torsion stiffness in the inner portion of the spar to provide pitch angle motion by twisting the spar, yet also provide a high bending stiffness to meet requirements in the flapwise and inplane directions. A comparison of the ratio of torsion and bending modulus for several types of materials illustrates the advantages of graphite for the flex beam spar application, Figure 32. The high bending modulus of graphite is utilized to obtain a blade inplane frequency greater than one per rev and separation of critical blade frequency to achieve aeroelastic stability.

Fiberglass and graphite composite are used for the aerodynamically contoured outer skin. The composite skin is molded into a cambered SC-1095 airfoil, and like the main rotor blades, uses a variable high twist to obtain the maximum aerodynamic performance. The blade twist is shown in Figure 33. Use of composite materials, which have a higher strain allowable than conventional metal materials, permits high speed operation with the high twist blade without a reduction in blade fatigue life. The high twist and advanced airfoil provide an improvement in rotor hover figure-of-merit from .68 for conventional tail rotors to .71.

R&M is improved in the crossbeam composite tail rotor by a reduction in the MTBF rate from 8.6 failures per 1000 hours to less than 4.9 for the UH-60A. This improvement is attributed to elimination of the pitch and flap bearings, use of corrosion resistant materials and the inherent damage tolerance

and ease of repairability of the composite construction. The improvements in performance and R&M are obtained in the crossbeam rotor without a corresponding increase in rotor system weight.

Prior to the first flight of the YUH-60A the tail/pylon assembly was thoroughly tested in the UTRC 18' wind-tunnel. The tail rotor had already been extensively tested on the whirl stand so the basic stability of the new crossbeam design had been demonstrated. The purpose of the tunnel test was to substantiate the stability of the fully coupled rotor/control system/tail pylon over the anticipated flight envelope.

A view of the tail rotor/tail pylon assembly mounted in the wind-tunnel is shown in Figure 34. Stability tests were conducted using an electromechanical shaker mounted on the tail pylon support structure which provided sinusoidal excitations of the tail rotor in both the inplane and out of plane directions. Natural frequencies and damping of critical system modes were determined from the resonant responses of the tail rotor.

The test envelopes which were explored in the wind-tunnel are shown in Figures 35 and 36. The envelopes included rotor speeds from 90% N_R to 125% N_R , airspeeds up to 160 knots (the tunnel limit) and sideslip angles from -20° to $+20^\circ$. The stability of the system was excellent throughout the wind-tunnel test envelope. Figures 37 and 38 present the measured frequency and damping of the critical rotor edgewise mode over the impressed pitch range up to airspeeds of 160 knots. These data are typical of the results obtained over the full test envelope. The damping of the rotor first edgewise mode was generally invariant with test condition and impressed pitch, remaining in the vicinity of 1-1/2% critical for all conditions. This confirmed that the design criteria of avoiding destabilizing couplings had been successfully achieved. The low variation in edgewise frequency with impressed pitch is a result of the pretwisted flexbeam which located the maximum edgewise stiffness at a point midway in the pitch range rather than at zero pitch.

The excellent stability characteristics of the bearingless tail rotor result in a large measure from two design features. First the critical flatwise and edgewise modal frequencies are well separated. This is accomplished by mounting the outer blade (airfoil) at an angle to the flexbeam axis so that the inplane stiffness at high blade pitch is increased, Figure 39. This design feature is unique to Sikorsky and is covered by a recently issued patent.

The second feature contributing to stability involves controlling the potential pitch-bending coupling that can exist on bearingless rotor designs, Figure 40. Although such couplings may eventually be controlled to advantage, at the present time they represent a significant risk area. We avoided this risk by constraining the inboard end of the torque tube with an elastomeric snubber, Figure 41. This provides a more direct path for reacting the shear forces generated by the control inputs. The resulting configuration has been exceptionally stable.

Canting the UH-60A tail rotor to provide a lift component at the tail permitted shortening of the nose to meet C-130 transportability dimensions. An upward cant of 20 degrees provides a 400-pound tail rotor lift component. This lift produces a tail-up moment that permits the nose to be shortened about two feet from what would otherwise be needed to balance the aircraft, Figure 42. In addition to shortening the aircraft, the lifting tail improves overall lifting efficiency and reduces the size, weight, and cost of the UH-60A. Tail rotor power is increased only 6%, or about 10 HP, by the small increase in tail rotor thrust required as a result of canting and the corresponding 10 HP reduction of the main rotor power reduces main rotor lift only 50 pounds. A net lift increase of 350 pounds is achieved for the same total power, Figure 43. The resulting 3% increase in overall system figure-of-merit permits a 14% smaller rotor, 6-1/2% (1,000 lb.) lower gross weight, and 7-1/2% (\$ 90,000) lower acquisition cost.

Flight Control

The UH-60A uses a stabilator to provide inherent longitudinal stability at high speed, Figure 44. It is an active device which has a varying incidence angle between the limits of 40 degrees leading edge up and -8 degrees leading edge down. Feedbacks from the speed sensor, collective stick, pitch rate gyro and lateral accelerometer alter the incidence, improving the longitudinal stability characteristics provided by the 45 ft² area.

Through the velocity feedback, the stabilator has been used effectively to improve the speed stability (longitudinal static stability). In addition, it decouples the collective-to-pitch motions which most single-rotor helicopters possess at the higher speeds through the use of the collective stick feedback. The pitch rate feedback to the stabilator has the primary effect of augmenting the aircraft pitch damping in cruise and a secondary effect of providing a positive maneuver stick position gradient throughout the c. g. envelope. Improvement in stabilizing the aircraft in gusty conditions is provided by lateral acceleration feedback. These features are covered in more detail in the following paragraphs.

Airspeed is sensed to control the stabilator incidence for low vertical drag in hover and to provide proper trim in forward flight and autorotation. In the low speed range from hover to 30 knots, the stabilator incidence is set at + 40 degrees. This feature reduces nose-up attitudes during transition to hover and improves fuselage attitude as well as pilot visibility during low speed flight.

As the UH-60A, at design weight, flies out to higher speeds, the stabilator incidence is reduced until it reaches a value of zero at approximately 80 knots. The stabilator stays at this value out to V_{max} . The zero degree stabilator incidence provides the lowest aircraft drag possible while still maintaining longitudinal control margins within desired limits.

When the UH-60A enters autorotation, lowering of the collective stick lowers the stabilator incidence to negative values. At 80 knots, a value of -5 degrees is reached. The negative incidence setting gives the aircraft comfortable pitch attitudes in descent and provides the pilot with adequate aft longitudinal stick margins.

The variation of stabilator incidence with forward speed and collective stick position is shown in Figure 45.

Lateral acceleration is sensed at the tail to eliminate yaw-to-pitch coupling. Because of the canted tail rotor, there is a pitching moment generated with sideslip which can be decoupled with the active stabilator. While pitching moments induced by tail rotor collective pitch changes are balanced out by a mixing of tail rotor-to-longitudinal cyclic pitch, external inputs such as generated by gusts and sideslip are not. For this coupling, a lateral acceleration signal, drives the stabilator to balance out this pitching moment. This decoupling has been achieved by locating the sensors at the nose of the aircraft to provide an effective lead to the signal.

During level flight and particularly in descending flight the vertical, and to a lesser extent the horizontal, stabilizer have to operate in the disturbed flow shed by the rotor hub and the aft pylon. The resulting low frequency vibration, tail shake, was effectively reduced by controlling the flow over the aft pylon, keeping the flow attached, and redirecting the resulting wake below the stabilizers. In earlier Sikorsky aircraft this was achieved by the use of a beanie, on the S-61, and by a "horse collar" pylon on the S-61 and S-65 series aircraft. On the UH-60A a lifting aft pylon, Figure 46 produced reductions in tail induced cockpit lateral vibration from 0.2 down to 0.03 'g'.

Airframe

Advanced composite materials are used in a number of important airframe elements on the UH-60A, as shown in Figure 47.

The canopy enclosure is an all-fiberglass structure utilizing skin-skeleton construction. In this design, the skeleton is molded using an integrated one-piece unit containing all sills, parts, and frames. The skin is layed-up and cured in a matched mold, and the two-pieces are then bonded together to form a complete assembly, ready for installation, Figure 48. Fabrication hours, normalized on a per-pound basis, are drastically lower for this design than sheet metal construction or conventional fiberglass construction methods.

Boron/epoxy material is used for stiffening purposes in the horizontal stabilator and cockpit understructure. In order to preclude dynamic resonance with the main rotor blades, it was necessary to provide flexural moments of inertia for these structures substantially greater than those required for strength. Boron epoxy was selected because of its high specific stiffness to weight ratio, and its compatability with conventional riveting assembly methods. Weight savings in the stabilator and cockpit beams were 22 pounds.

Kevlar/ epoxy is also used extensively in the airframe for doors, fairings and secondary structures. The entire main rotor pylon is Kevlar/ epoxy sandwich structure.

Unidirectional fiberglass/Nomex floors are to be used in the production UH-60A's to achieve superior dent resistance in an all-composite floor.

Based on a thorough development program the S-76 helicopter has incorporated in its construction a substantial amount of composite material such as Kevlar, graphite, and glass epoxy laminates, Figure 49.

Kevlar fabric is used to great advantage to minimize weight of secondary structural components such as doors, access panels and fairings. To suit the particular need, Kevlar material is laid up in a prepreg laminate or used as the skin covering in a single stage cure cycle honeycomb sandwich panel. Resin systems are selected to minimize property degradation due to heat and moisture.

The canopy is fabricated from molded fiberglass in a two stage cure cycle operation. The skin and skeleton assemblies are cured separately and then bonded together to form the entire canopy structure. Unidirectional "s" glass is used in corner post areas to increase stiffness strength.

The S-76 also features a horizontal stabilizer made entirely of advanced composite laminates, Figure 50. The skins are Kevlar/epoxy Nomex honeycomb core, with graphite/epoxy spar caps and a Kevlar/epoxy torque tube. The stabilizer represents the first primary production component made from advanced composite materials scheduled to be approved by the FAA in the type certification of a transport rotary wing aircraft.

Advanced composites provide substantial payoffs to the airframe and stabilizer of the S-76. For the airframe components affected a 30 percent weight savings was achieved.

Survivability Characteristics

During the 60's, the Eustis Directorate of the U. S. Army Air Mobility Research and Development Laboratory contracted with the Aviation Crash Injury Research (AvCIR) Group of the Flight Safety Foundation to define the Army aircraft crash environment and develop design concepts and criteria to reduce injuries.

That document was used from the outset in design of the U. S. Army/ Sikorsky YUH-60A utility helicopter to meet the Army requirements.

Technology Payoffs

What were the payoffs of the application of advanced technology to the UH-60A and S-76 helicopters?

In the foregoing discussion selected major areas of technological advances have been presented. However it is not possible in one paper to do justice to the total accomplishment made in bringing forward this new generation of helicopters. The past decade saw a major change in design philosophy and priorities which impacted heavily on factors which influence the operator's cost of ownership — acquisition and life cycle cost. This was a period of cost consciousness which introduced cost factors as prime variables in the design equation. It was no longer sufficient or proper to design a system with emphasis on exceeding performance objectives but rather to meet the requirements with a solution that would result in achieving cost targets. The establishment of cost goals was a major innovation.

Cost goals were achieved by bringing together the engineering, manufacturing, quality control, purchasing and product support disciplines to achieve a sum total lowest cost through judicious compromise — and yet meet all of the customer's requirements. Some components were redesigned several times to meet cost targets and in some instances the lowest cost design turned out also to have lower weight — a most welcome result.

Other contributors to cost reduction are the broad use of computer-aided design and manufacturing techniques and use of advanced flight test data acquisition and processing systems to reduce test time and cost.

The achievement of high reliability and maintainability was also a major payoff. This resulted from simplified components, improved inspectability and on-condition replacement of components. The composite titanium spar blade was designed to operate at stress levels low enough to eliminate the need to specify a replacement time. The elastomeric rotor resulted in a 70 percent reduction in parts count. The use of highly reliable elastomeric bearings requiring no lubrication and readily inspectable for condition, reduced the maintenance burden. Similarly, the development of the bearingless, graphite tail rotor provided large increases in reliability and maintainability.

The main transmission was designed to achieve improvements of both reliability and maintainability. The UH-60A main gear box uses 38% fewer parts, 42% fewer bearings, 32% fewer gears, 80% fewer seals and half the number of free wheel units compared to the current production S-61. The gear box consists of five modules which are disassembled with a single standard wrench. Left hand and right hand modules are interchangeable. It uses an integral lubrication system and individual chip detectors for ease of fault isolation and maintenance. The gear box will operate for over one hour in cruise flight after loss of oil. The use of advanced digital automatic flight control systems also contributed to a major improvement in R&M at the same time reducing weight and volume.

The technology payoff in reliability was the ability to exceed Army requirements. Reliability is summarized in the following table:

UH-60A RELIABILITY

Mission Reliability	.988306
Safety Reliability	.999976
Mean Time Between Failure, Hours	4.5
MTB Maintenance, Hours	2.89
Component MTB Removal, Hours	1754—4751

This represents a 4.75 : 1.0 improvement in reliability compared to prior helicopters.

The advanced technology also paid-off in exceeding maintainability requirements. The following table summarizes the UH-60A values:

UH-60A MAINTAINABILITY

Mean Time to Repair, Hours	0.73
Corrective MMH /FH (all levels)	2.84
Fault Corrective MMH/FH	0.40
On Aircraft Corrective MMH/FH	0.40
Inherent Availability	0.984

This represents a 9.0 : 1.0 reduction in maintenance compared to previous aircraft.

Dramatic technology payoffs were realized in the S-76:

As shown in Figure 51 the S-76 range carrying 12 passengers at S. L. 90° F conditions is twice that of 1965 helicopters.

The fuel consumed has been reduced 50 percent. At the same time the cruise speed has gone up by 25 percent to 145 knots, Figure 52.

Maintenance man-hours per flight hour have been cut by 40 percent, or from 5 hours in 1955 to an estimated 3 hours for the S-76, Figure 53.

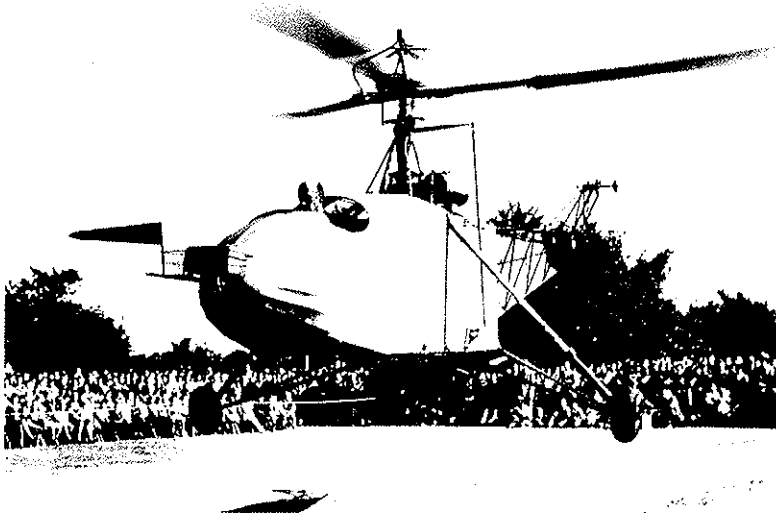
The weight empty to gross weight ratio has been dramatically reduced from 66 percent for 1955 helicopters to less than 51 percent for the S-76, resulting in an overall improvement of 23 percent, Figure 54.

The operating cost per passenger seat mile will drop 50 percent from 32 cents in 1955 to an estimated 16 cents for the S-76, Figure 55.

The technological advancements applied to the UH-60A and S-76 have ushered in a new era of helicopter efficiency and effectiveness. As we go into production of these systems we look forward to the next generation of aircraft which, with similar emphasis on research and development, will achieve as remarkable an improvement in attributes as we have achieved in the UH-60A and S-76. Broader use of composite materials and higher strength metals, use of miniaturized solid state electronics and advanced cockpit displays, fuel-efficient engines and power control systems, advanced transmission housings and components will bring us to the next level of accomplishment.

Reference (a): Gormont, Ronald E. and Wolfe, Robert A. ,
U. S. Army Aviation Systems Command, the U. S. Army
UTTAS and AAH Programs. Presented at AGARD Rotorcraft
Design Symposium, Moffett Field, California, U. S. A. ,
May 1977.

VS-300



SIMULATOR

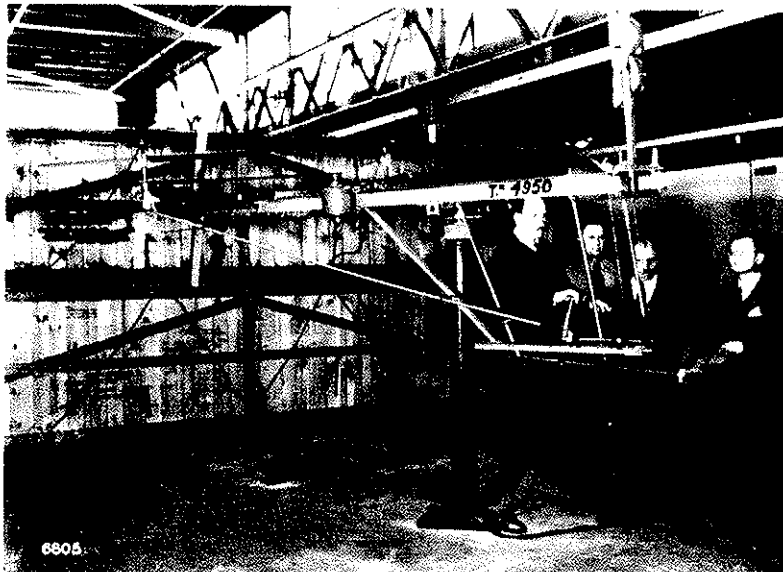


Figure 2

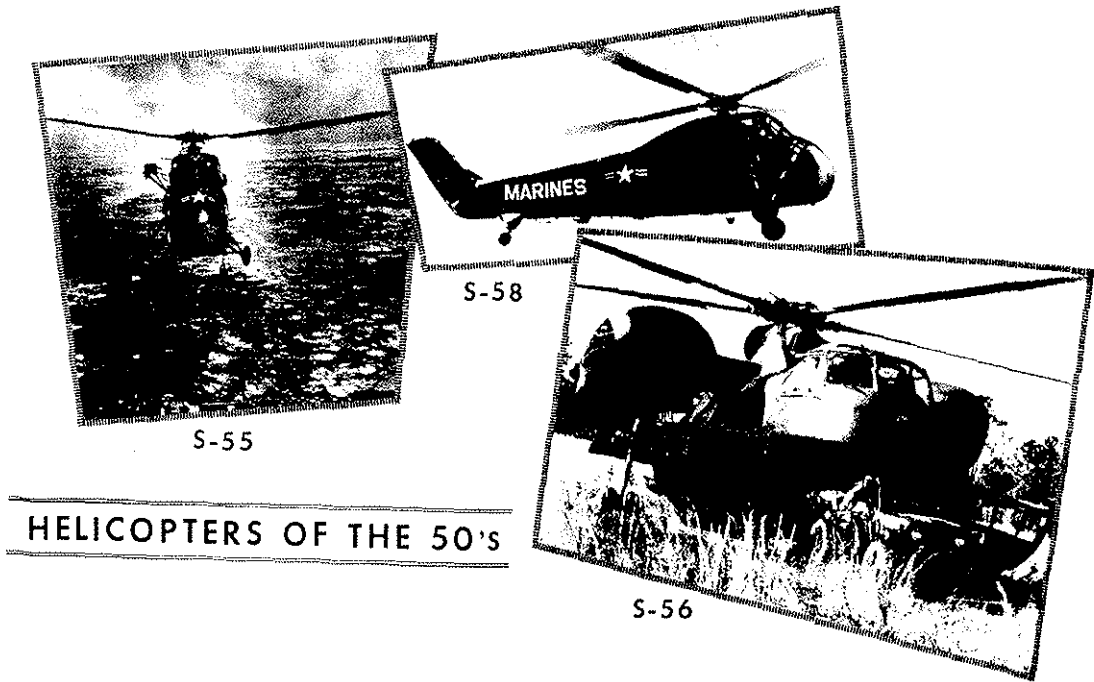


Figure 3

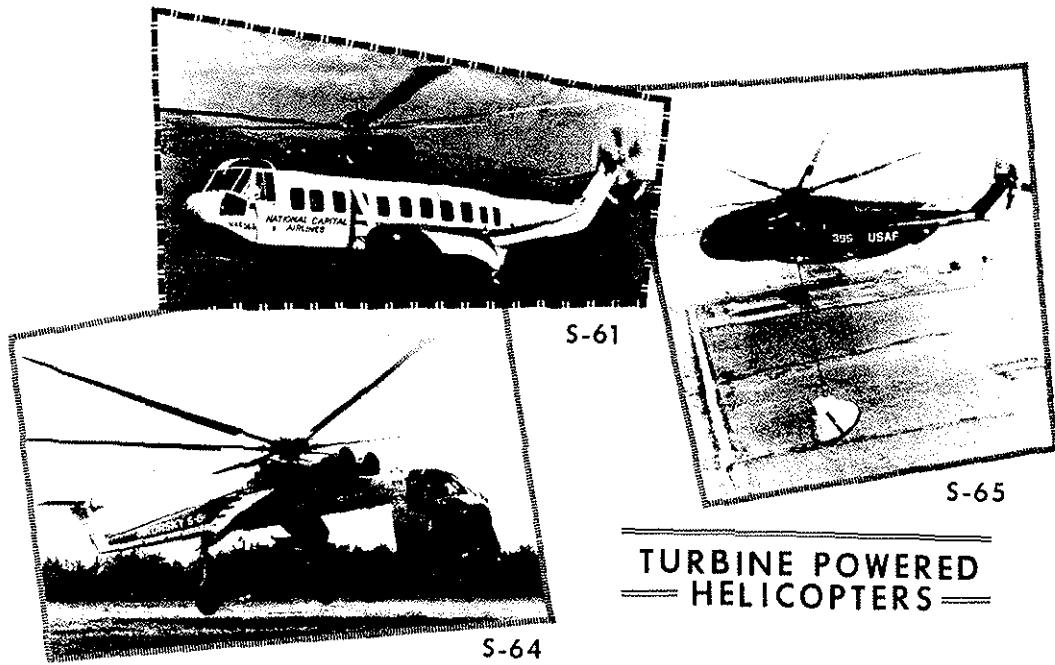
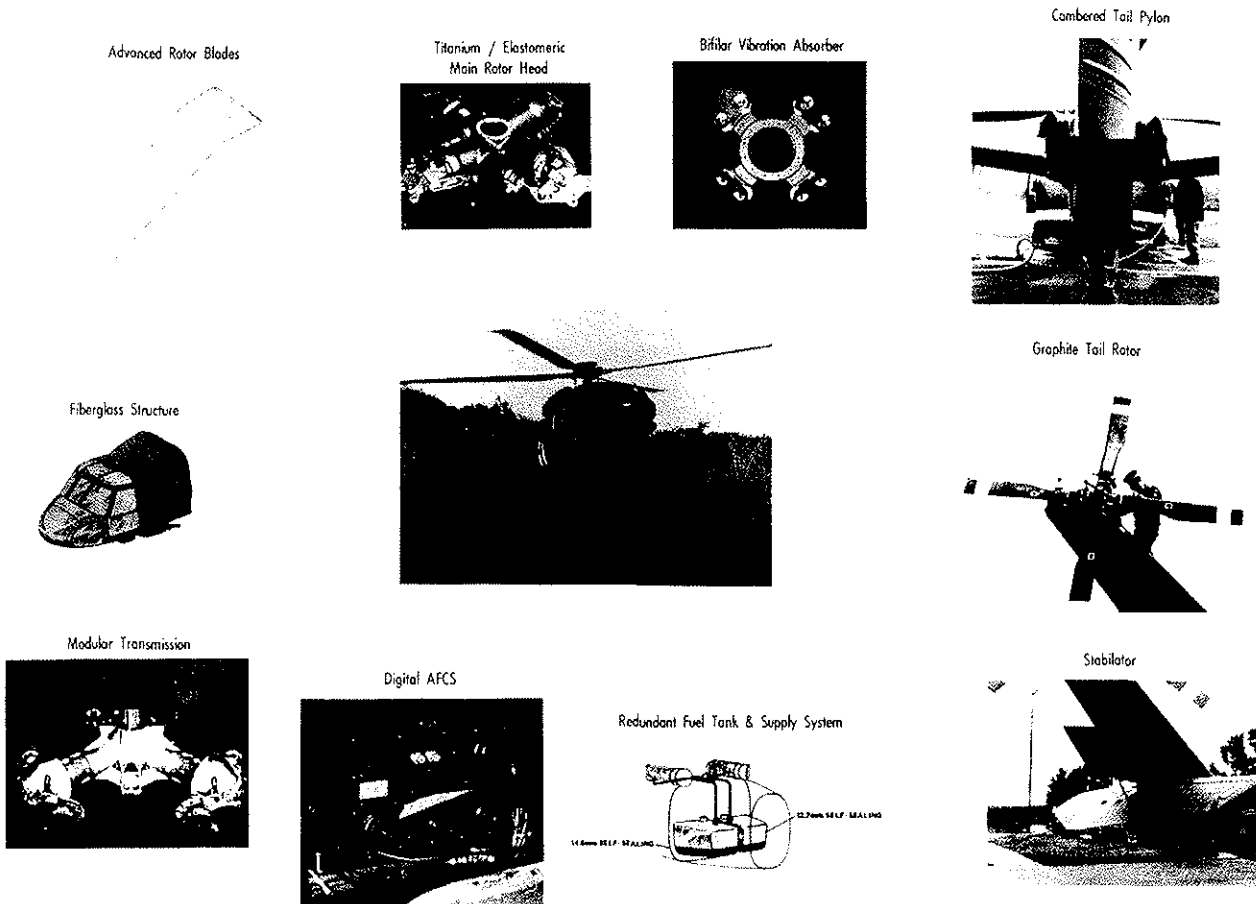


Figure 4



S-76 TECHNOLOGY FEATURES

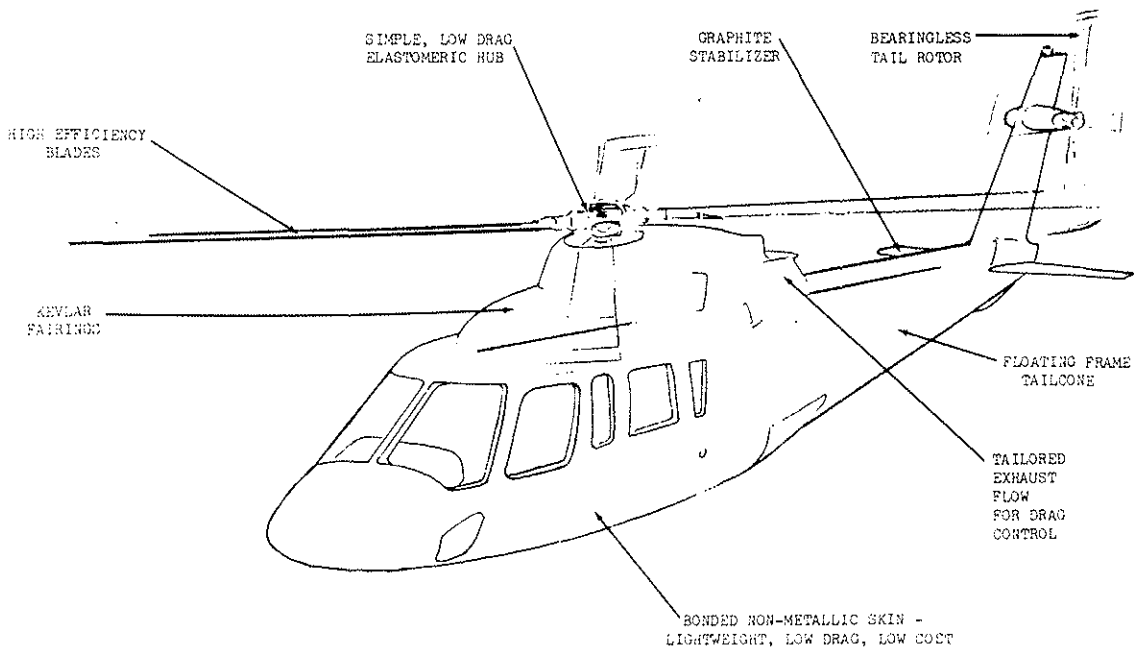


Figure 6

The 1000+ POUND EXTRA LIFT OF THE
UTTAS BLADE PAYS FOR:

* IR Suppressor.	314 Lbs
* Crashworthy Fuel System.	164 Lbs
* Ballistic Tolerance.	125 Lbs
* Deicing	79 Lbs
* Additional Payload	393 Lbs
	1075 Lbs

Figure 7

SCHLIEREN FLOW VISUALIZATION
OF THE WAKE OF A HOVERING ROTOR

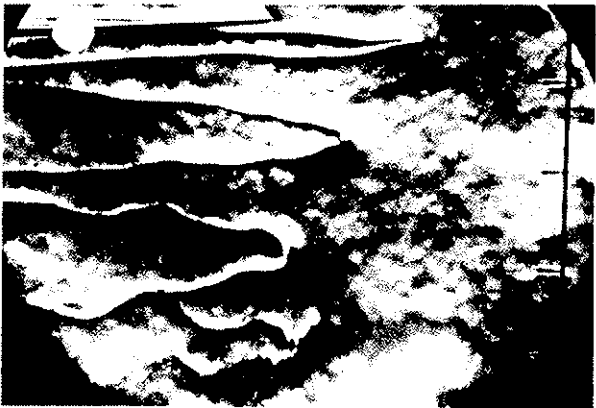


Figure 8

MODERN ROTOR AERODYNAMICS
TECHNOLOGY IMPROVES FIGURE OF MERIT

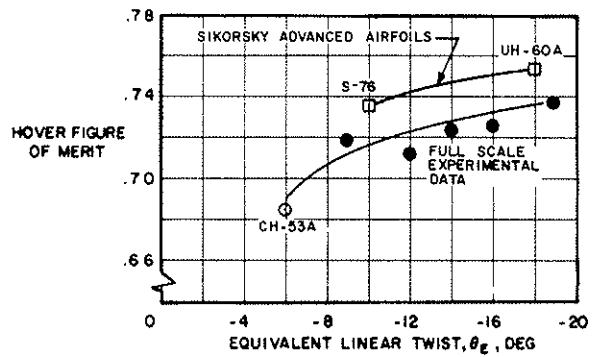


Figure 9

EFFECT OF THE INFLOW ASSUMPTION ON CALCULATED ANGLE OF ATTACK DISTRIBUTION

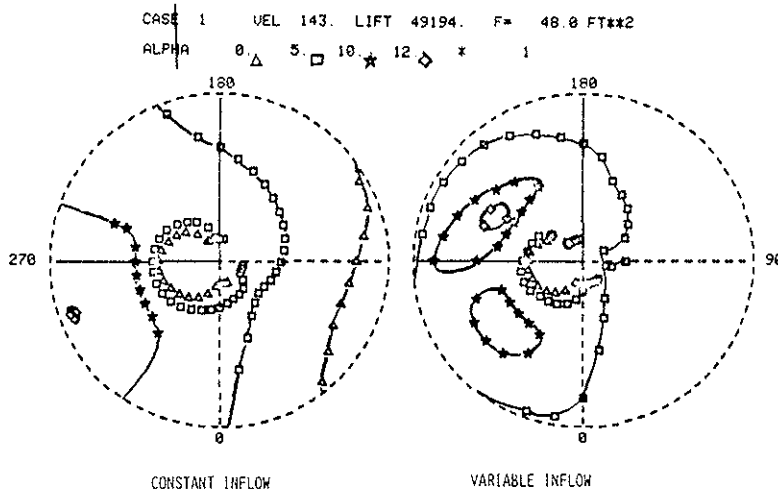


Figure 10

A COMBINATION OF NEW AIRFOILS WAS USED TO MEET PERFORMANCE OBJECTIVES

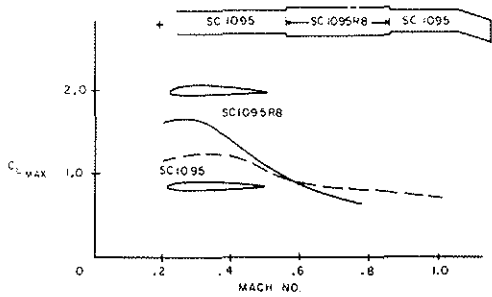


Figure 11

GROSS WEIGHT - SPEED ENVELOPE IMPROVEMENT OF THE UH-60A

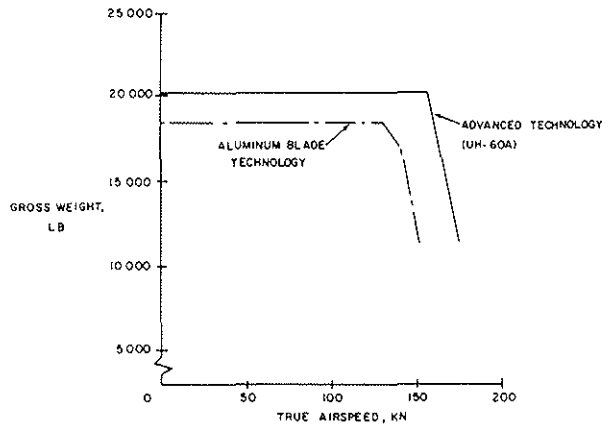


Figure 12

SOURCE OF DESTABILIZING PITCH MOMENT DUE TO TWIST

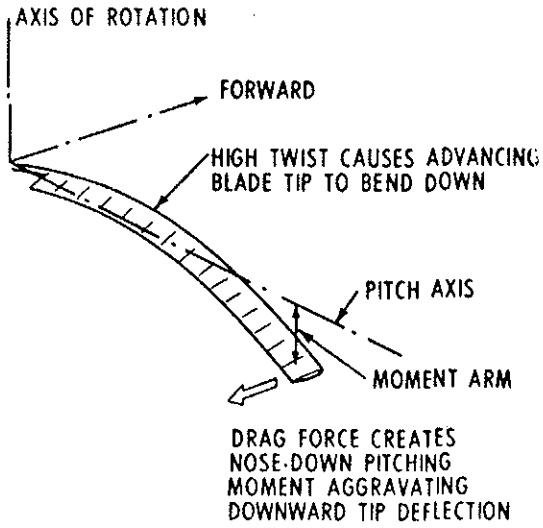


Figure 13

EFFECT OF TIP SWEEP ON CONTROL LOADS

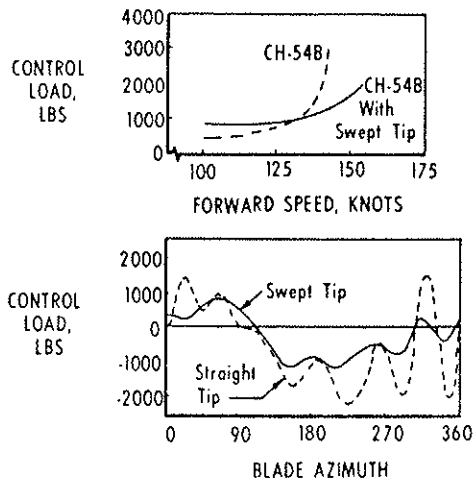


Figure 14

AFT TIP SWEEP IS EFFECTIVE IN CONTROLLING TORSIONAL RESPONSE

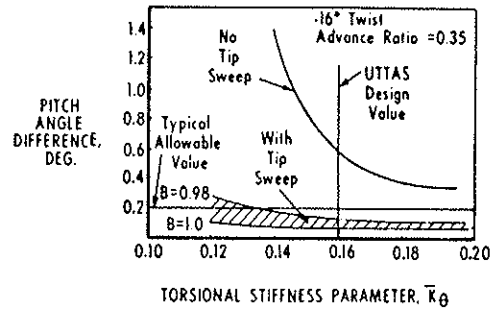
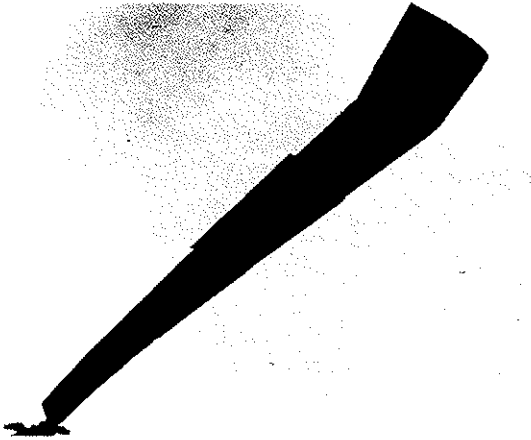
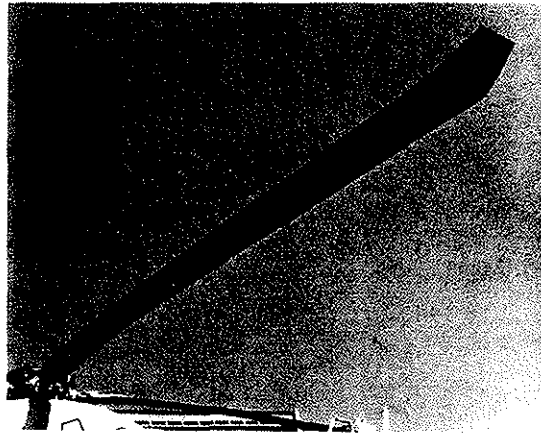


Figure 15

UH-60A MAIN ROTOR BLADE



S-76 MAIN ROTOR BLADE



EFFECT OF TIP SHAPE ON ROTOR PERFORMANCE

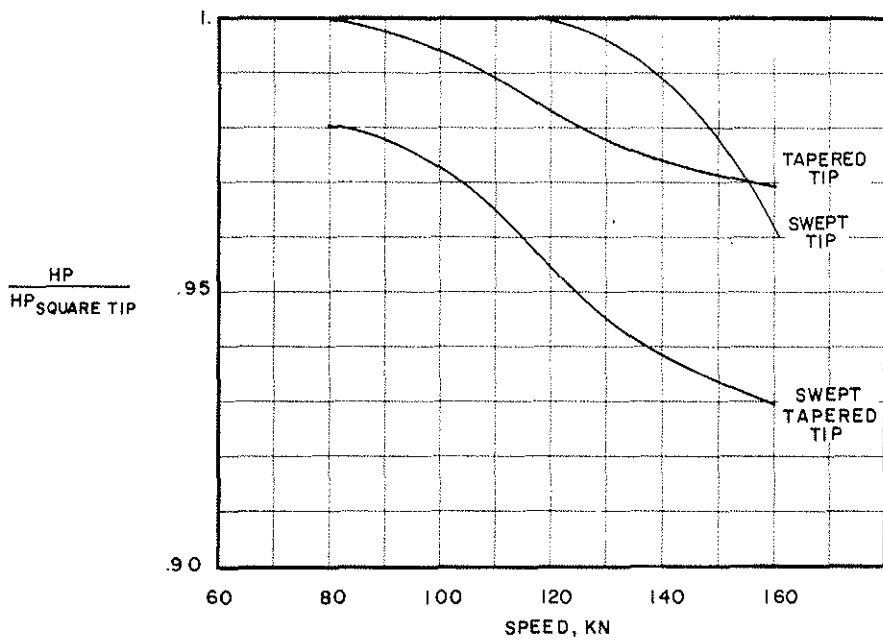


Figure 18

TITANIUM/COMPOSITE UH-60A BLADE

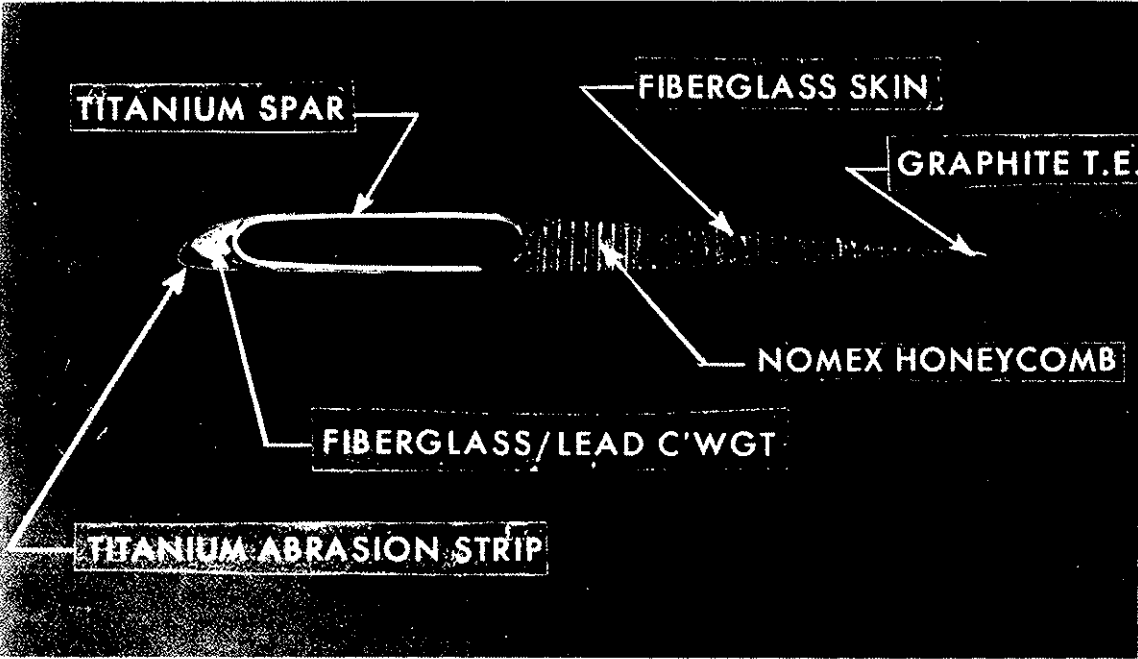


Figure 19

EFFECT OF BLADE TWIST ON VIBRATORY STRESSES

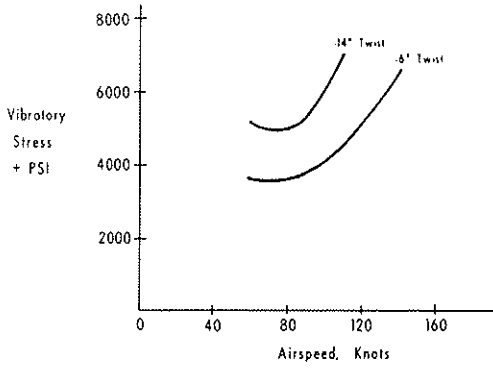


Figure 20

HIGH PERFORMANCE BLADES GENERATE MORE PITCHING MOMENT

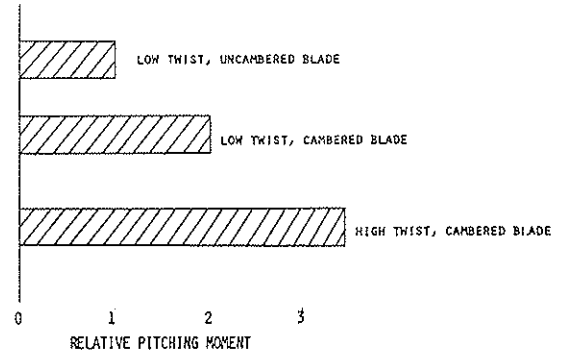


Figure 21

FIBERGLASS SPARS PRODUCE UNACCEPTABLE BLADE AEROELASTIC TWISTING

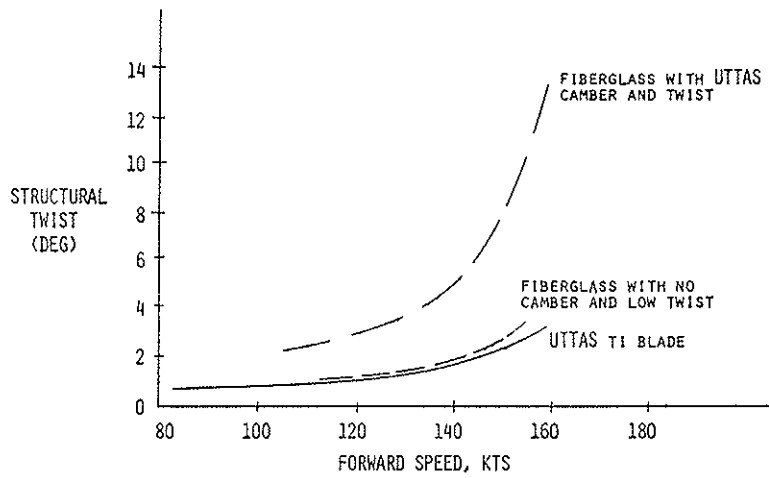


Figure 22

STRESS DERATING OF UTTAS TITANIUM SPAR IS KEY TO RELIABILITY

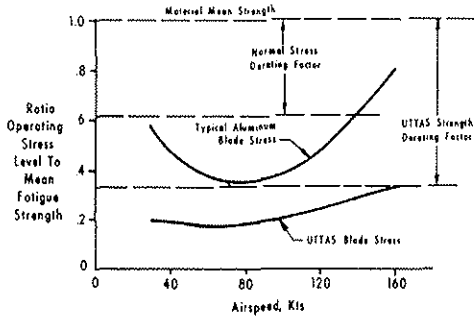


Figure 23

TITANIUM BLADE DESIGN FOR LOW RELATIVE STRESSES

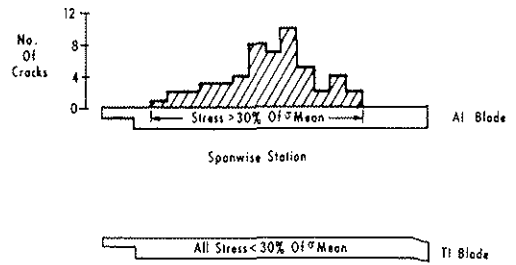


Figure 24

TITANIUM SPAR RELIABILITY UNAFFECTED BY GROSS MANUFACTURING FLAWS

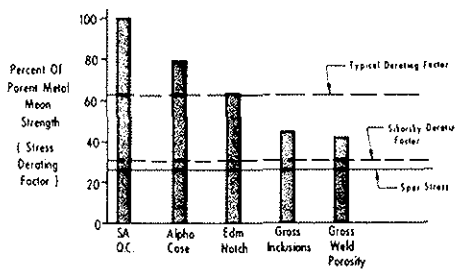


Figure 25

TITANIUM BLADE 23mm HEI HIT

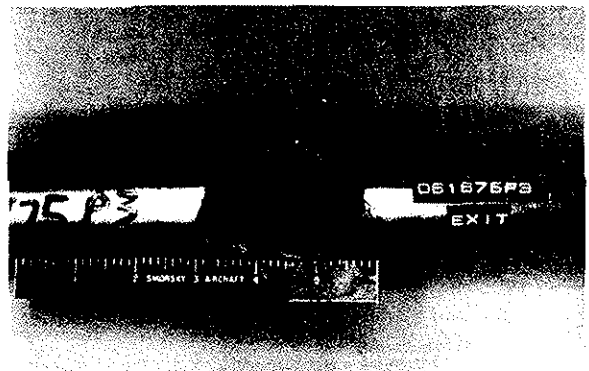


Figure 26

UH-60A ELASTOMERIC BEARINGS

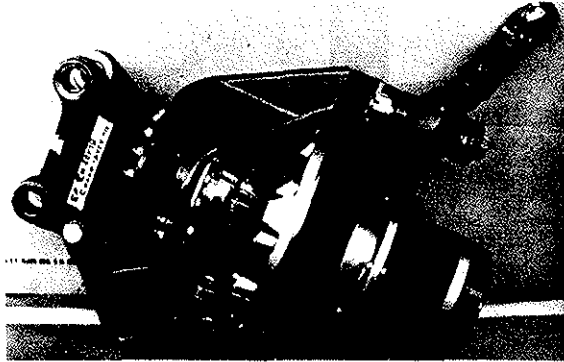


Figure 27

UH-60A MAIN ROTOR HUB

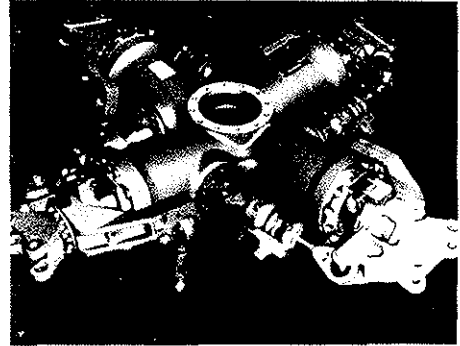


Figure 28

S-76 MAIN ROTOR ELASTOMERIC BEARINGS QUALIFICATION TEST

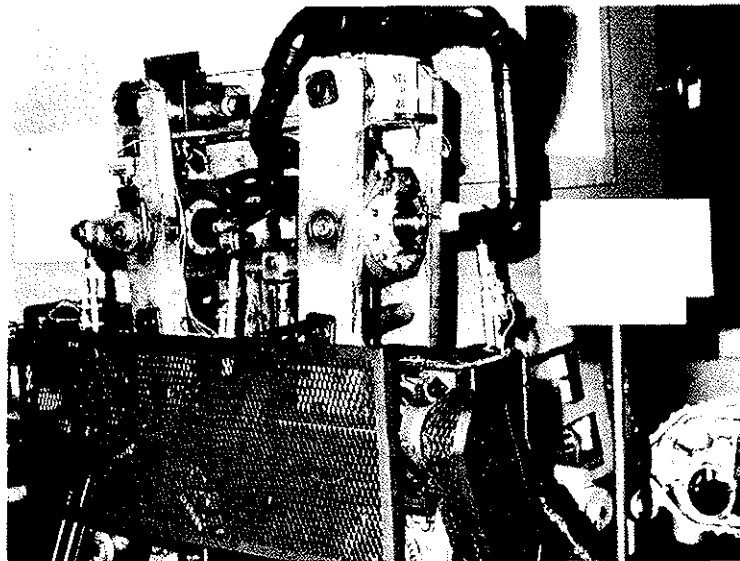


Figure 29

ARTICULATED ROTOR LAG DAMPER PROVIDES
ROTOR/DRIVE SYSTEM TORSIONAL MODE STABILITY

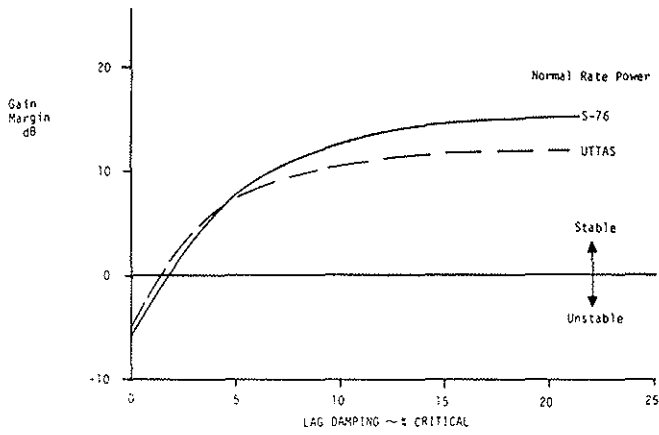
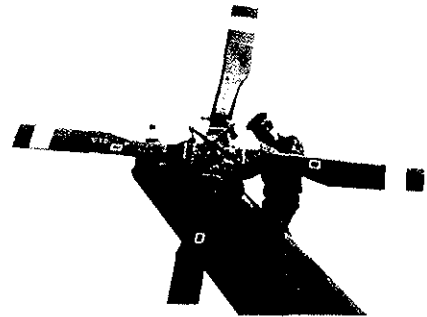


Figure 30

SIMPLE BEARINGLESS TAIL ROTOR



NO PITCH, FLAP OR LAG BEARINGS
30 FEWER PARTS

Figure 31

GRAPHITE COMPOSITE PROVIDES THE HIGHEST BENDING TO
TORSION MODULUS RATIO AT THE LOWEST WEIGHT

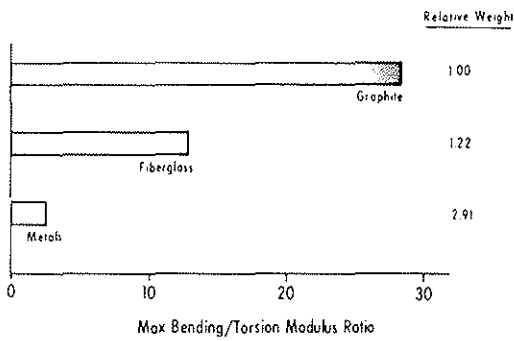


Figure 32

BEARINGLESS TAIL ROTOR SHOWING TWIST



Figure 33

UH-60A CROSSBEAM TAIL ROTOR WIND TUNNEL INSTALLATION

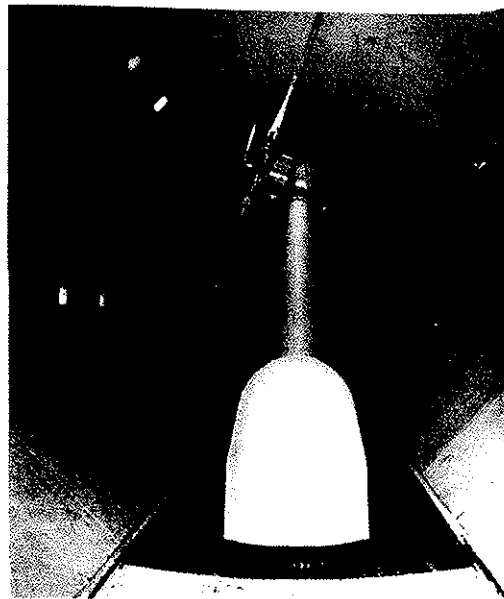


Figure 34

CROSSBEAM TAIL ROTOR
AIRSPEED, IMPRESSED PITCH,
ROTORSPEED WIND TUNNEL TEST ENVELOPE

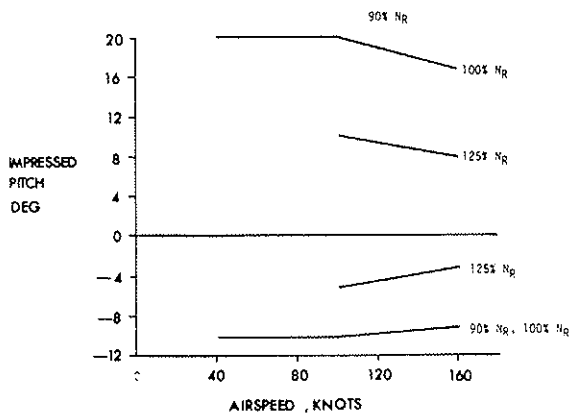


Figure 35

CROSSBEAM TAIL ROTOR AIRSPEED/SIDESLIP
WIND TUNNEL TEST ENVELOPE

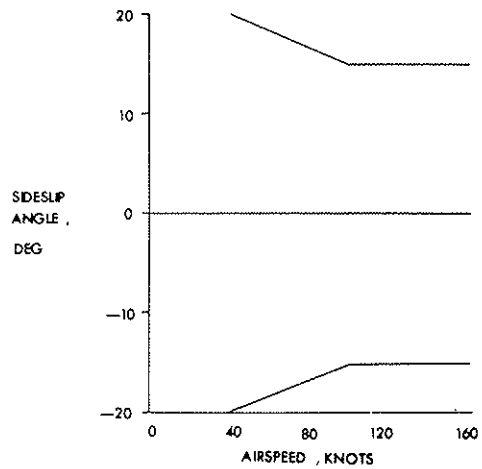


Figure 36

CROSSBEAM TAIL ROTOR EDGEWISE MODE DAMPING

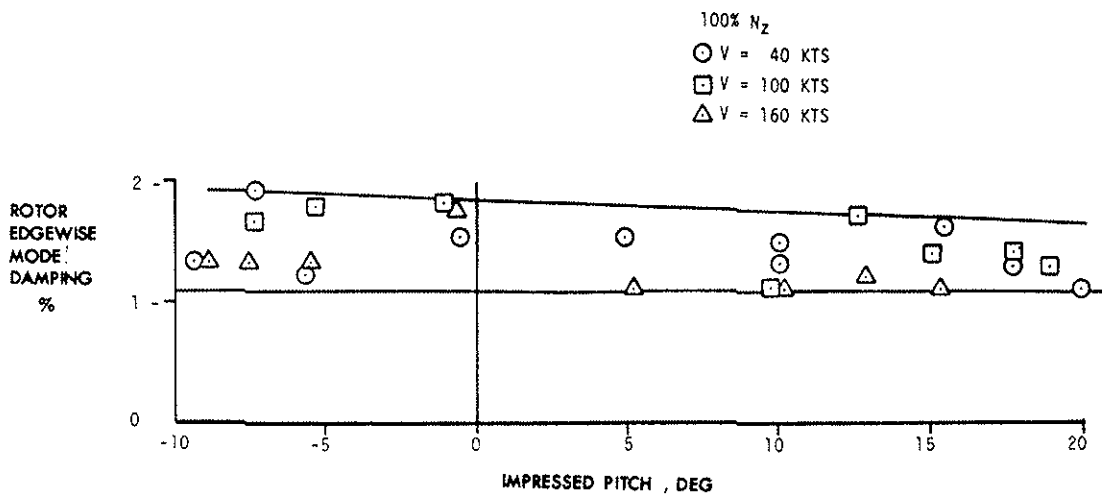


Figure 37

CROSSBEAM TAIL ROTOR EDGEWISE MODE FREQUENCY

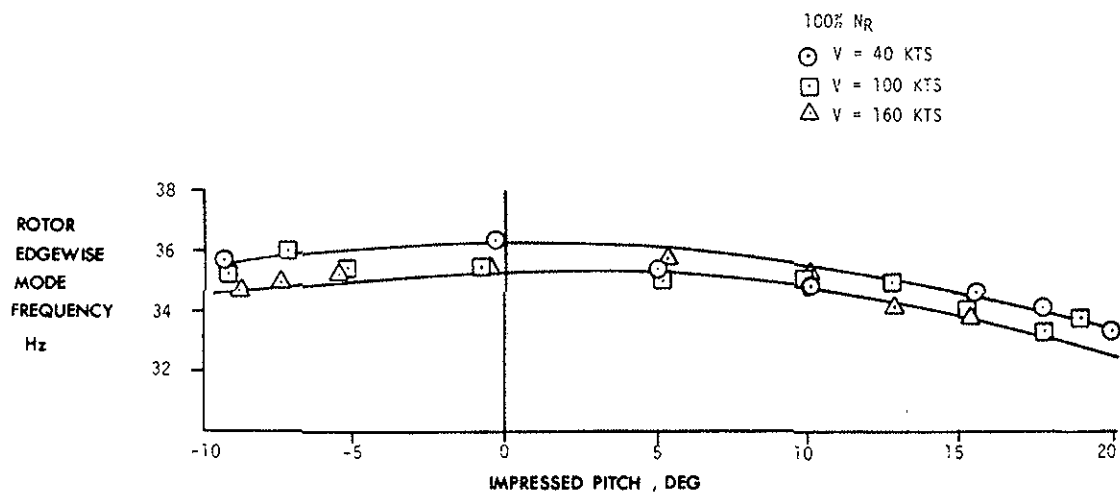


Figure 38

UNTWISTED FLEXBEAM PROVIDES SEPARATION OF FREQUENCIES OVER ENTIRE PITCH RANGE

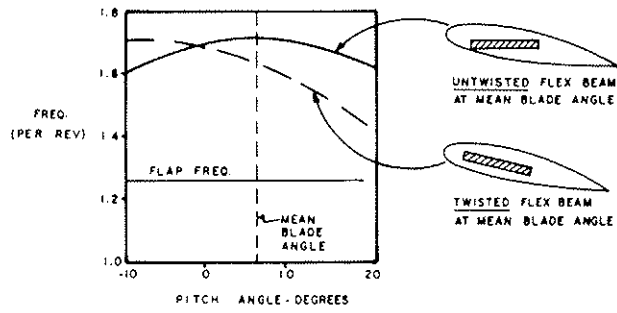


Figure 39

CANTILEVER TORQUE TUBE PRODUCES LARGE PITCH-BENDING COUPLING

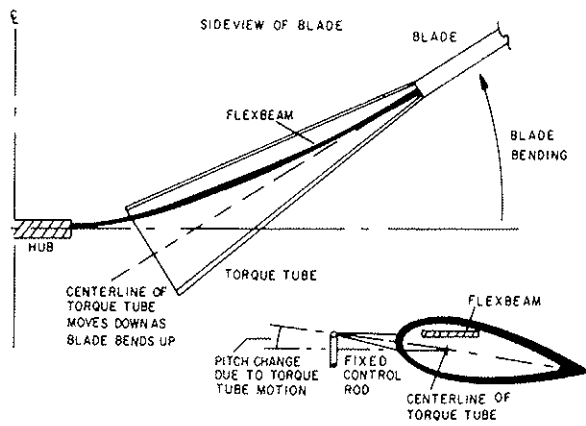


Figure 40

TORQUE TUBE SNUBBER ELIMINATES PITCH-BENDING COUPLING

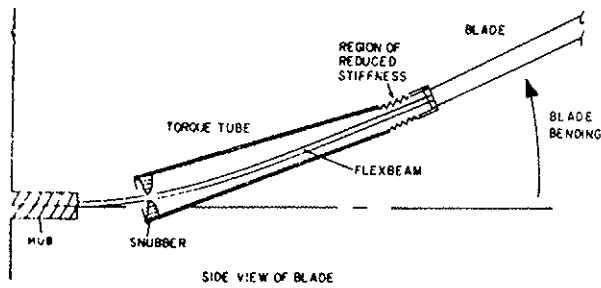


Figure 41

**CANTED TAIL ROTOR PERMITS A SHORTER NOSE
FOR BETTER AIR TRANSPORTABILITY**

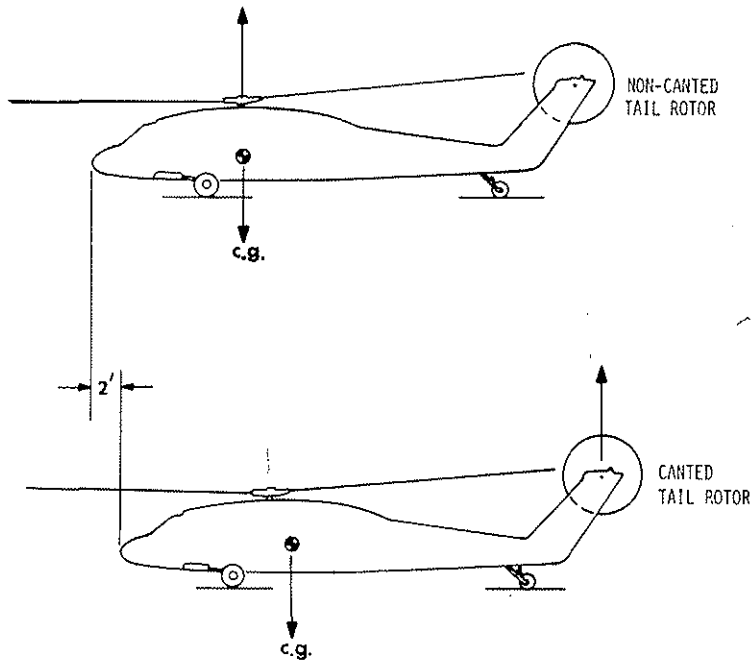


Figure 42

**TWENTY-DEGREE TAIL ROTOR CANT PROVIDES A
NET LIFT INCREASE OF 350 LB**

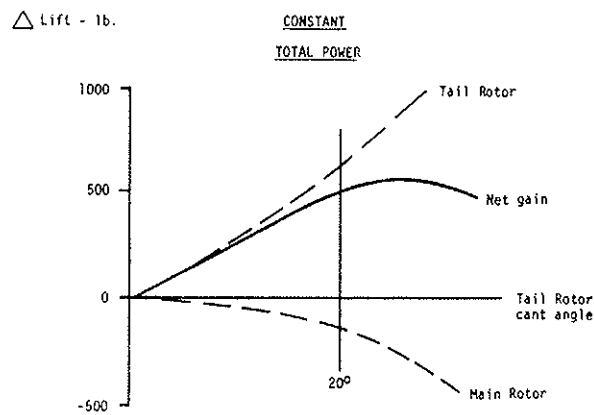


Figure 43

UH-60A STABILATOR

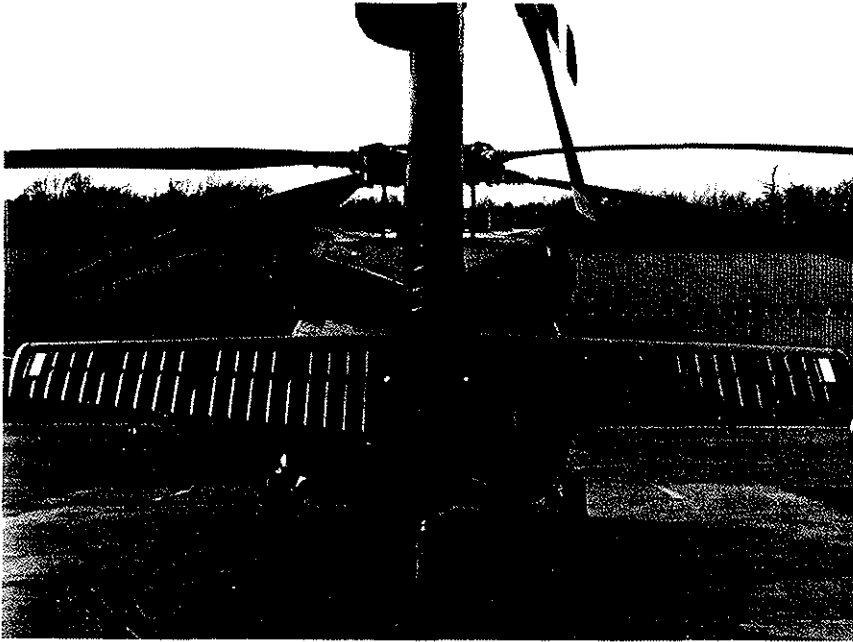


Figure 44

STABILATOR INCIDENCE VARIATIONS

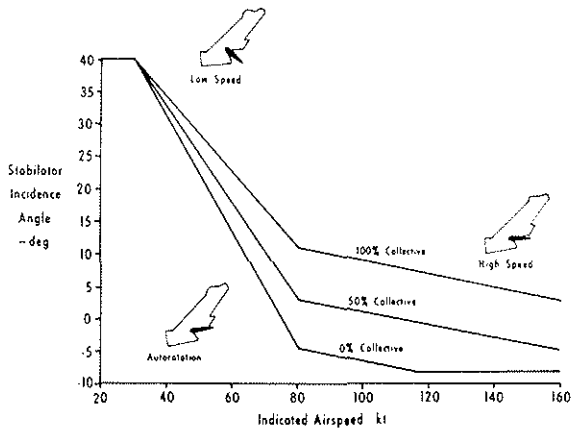


Figure 45

UH-60A WITH "LIFTING AFT PYLON FAIRING"



Figure 46

COMPOSITE USE ON UH-60A

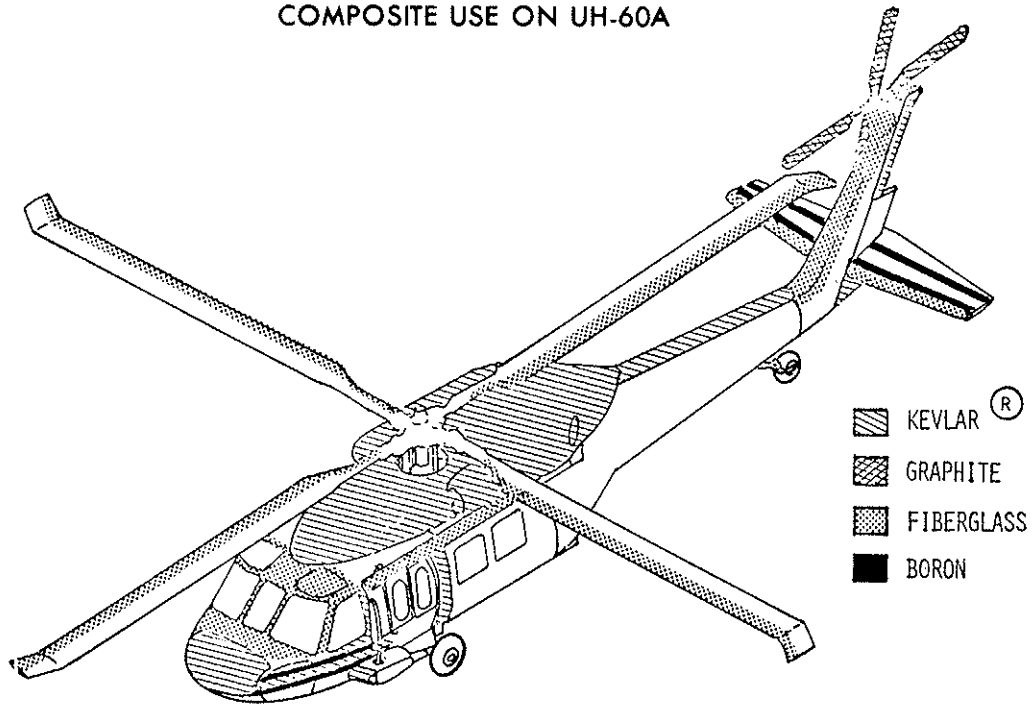


Figure 47

FIBERGLASS CANOPY ON UH-60A

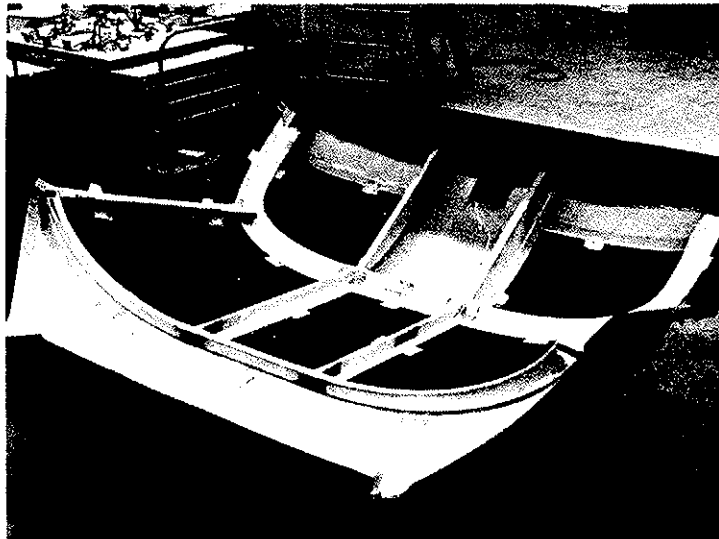


Figure 48

COMPOSITE MATERIAL APPLICATIONS , S-76 HELICOPTER

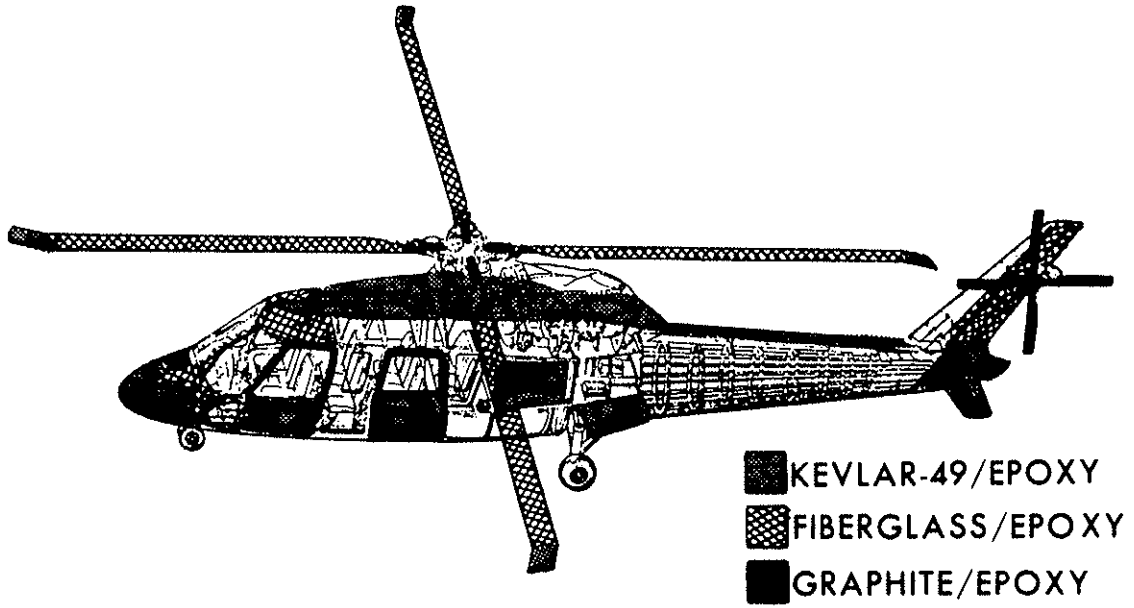


Figure 49

S-76 COMPOSITE STABILIZER

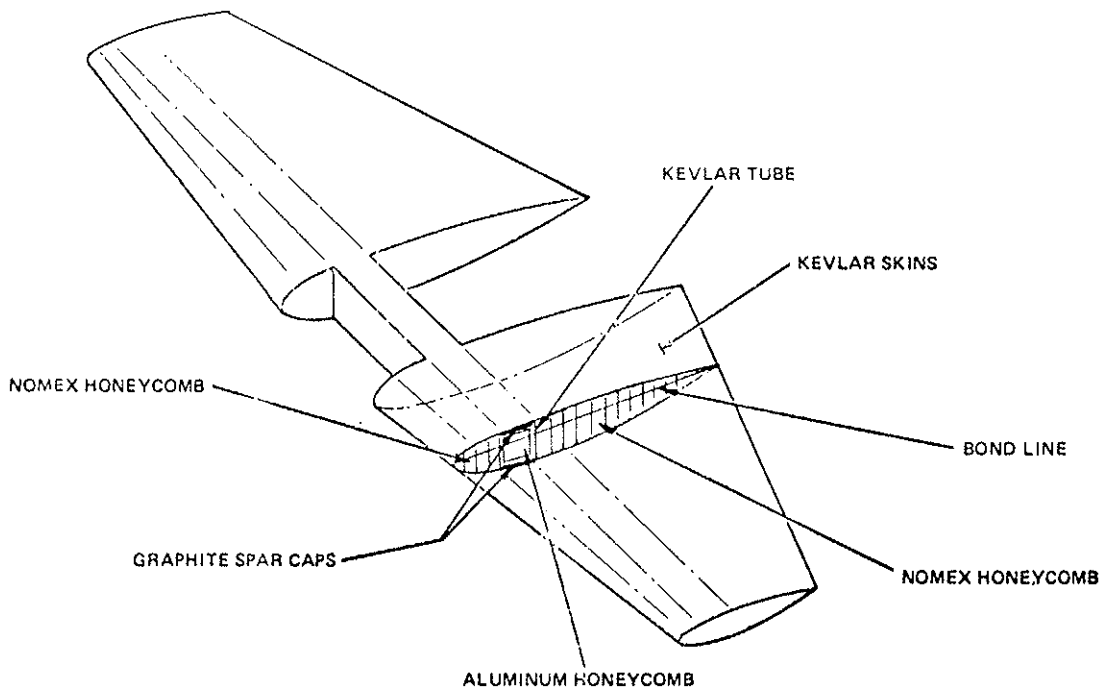


Figure 50

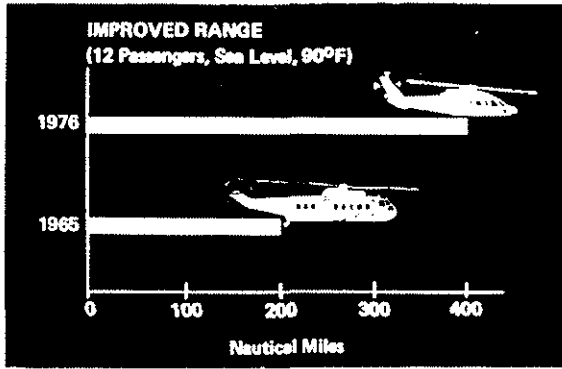


Figure 51

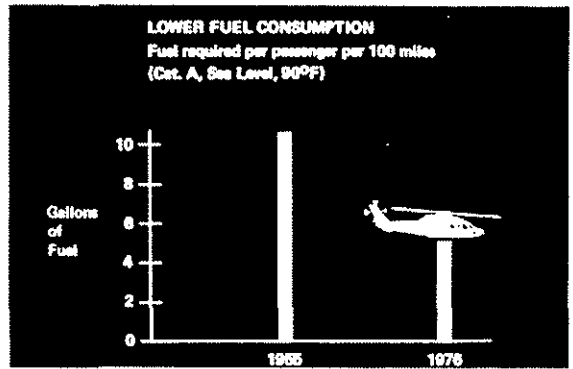


Figure 52

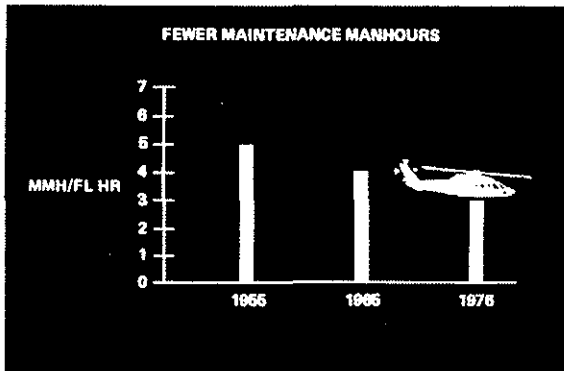


Figure 53

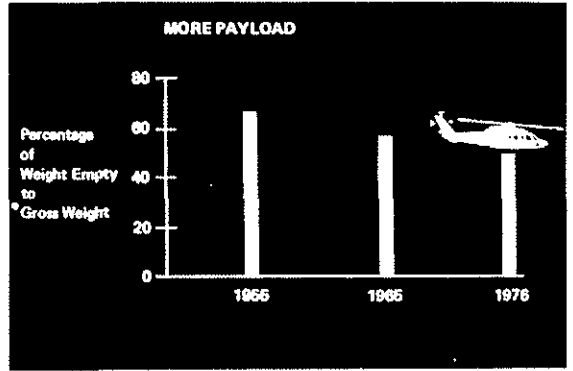


Figure 54

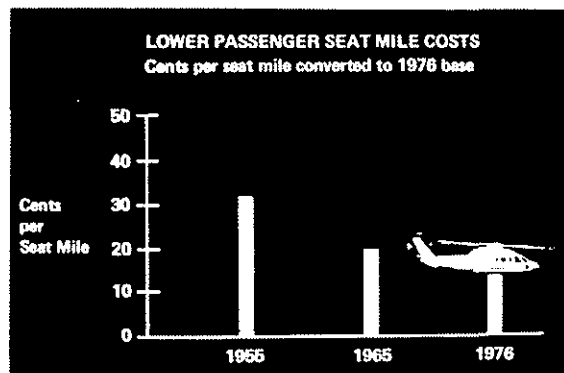


Figure 55